

A calpain unique to alveolates is essential in *Plasmodium falciparum* and its knockdown reveals an involvement in pre-S-phase development

Ilaria Russo, Anna Oksman, Barbara Vaupel, and Daniel E. Goldberg¹

Departments of Medicine and Molecular Microbiology, Howard Hughes Medical Institute, and Washington University School of Medicine, 660 South Euclid Avenue, St. Louis, MO 63110

Edited by Anthony Cerami, Warren Pharmaceuticals, Ossining, NY, and approved November 21, 2008 (received for review July 18, 2008)

Plasmodium falciparum encodes a single calpain that has a distinct domain composition restricted to alveolates. To evaluate the potential of this protein as a drug target, we assessed its essentiality. Both gene disruption by double cross-over and gene truncation by single cross-over recombination failed. We were also unable to achieve allelic replacement by using a missense mutation at the catalytic cysteine codon, although we could obtain synonymous allelic replacement parasites. These results suggested that the calpain gene and its proteolytic activity are important for optimal parasite growth. To gain further insight into its biological role, we used the FKBP degradation domain system to generate a fusion protein whose stability in transfected parasites could be modulated by a small FKBP ligand, Shield1 (Shld1). We made a calpain-GFP-FKBP fusion through single cross-over integration at the endogenous calpain locus. Calpain levels were knocked down and parasite growth was greatly impaired in the absence of Shld1. Parasites were delayed in their ability to transition out of the ring stage and in their ability to progress to the S phase. Calpain is required for cell cycle progression in *Plasmodium* parasites and appears to be an attractive drug target. We have shown that regulated knockdowns are possible in *P. falciparum* and can be useful for evaluating essentiality and function.

cell cycle | cysteine protease | essentiality | inducible | malaria

Plasmodium falciparum, the causative agent of severe malaria, has a complex life cycle involving numerous biological events, such as migration, host cell invasion, metabolism, and cell cycle progression and egress. Cysteine proteases have been implicated in most of these processes (1), but the function of many of the estimated 35 members of this protease class encoded in the genome has not been defined. Among them a single calpain-like protease is recognized (2).

Calpains belong to the C2 family of cysteine proteases. Calpains are found in organisms from bacteria to mammals and exhibit great divergence of sequence and domain structure but have homologous catalytic domains. Calpains have been implicated in diverse processes (3–6), such as muscle function, cell signaling, migration and attachment, death, transformation, cell-cycle regulation, differentiation and development, and fungal alkali tolerance, although the precise physiological role of many of these calpains is still poorly understood (3, 7).

Calpains can be divided into typical (resembling calpain 1) and atypical (lacking domain IV) (4, 5). In typical calpains, domain IV mediates Ca²⁺ binding and consequently activity regulation and dimerization (8). In *P. falciparum*, only 1 calpain gene (*Pcalp*) is apparent in the genome (2), and it is atypical. It has an unusually long coding sequence, and outside of the catalytic domain, has only distant homology with characterized calpains. We found that *Pcalp* contains several subdomains that are highly conserved in related species and confer uniqueness to the protein. One of them determines nucleolar localization, and another regulates calpain movement in and out of the nucleus through reversible palmitoylation (I.R., unpublished data). Surprised by the location of *Pcalp*, we

undertook a genetic characterization to assess its essentiality and gain insight into its function in the cell.

We report that *Pcalp* is a distinct type of calpain restricted to alveolates. Using multiple approaches, we show that the gene is essential to intraerythrocytic parasites. By developing a conditional knockdown system, we have been able to examine gene function. *Pcalp* plays a critical role in cell cycle progression during trophozoite development.

Results

***Pcalp* Is a Distinct Type of Calpain Restricted to Alveolates.** We identified a single calpain gene (*Pcalp*) in *P. falciparum*, MAL13P1.310 locus. The predicted coding region is 6,147 bp, encodes a 242-kDa protein, and was confirmed by extensive sequence analysis of the genomic DNA and cDNA amplified from mature mRNA (*SI Materials and Methods*). Orthologs to *Pcalp* were found in all *Plasmodium* species for which sequence data are available (Table S1). By phylogenetic analysis we confirmed that *Pcalp* has greatest homology to *Aspergillus* PalB (2), limited to the catalytic domain. However, the low reliability of its node derivation indicates substantial divergence (Fig. 1). In fact, aside from a central calpain catalytic domain (IIa-b) and a C-terminal domain homologous to calpain domain III, *Pcalp* possesses a long N terminus that has no significant homology to any known protein. *Pcalp* is a distinct type of calpain for its domain composition, not common to any other identified calpain class (Fig. 1).

All sequenced apicomplexan parasite genomes encode a single calpain with N-terminal homology, although for some of them the gene predictions result in a shorter encoded N terminus (Fig. 1). Two ciliate calpains, from *Tetrahymena* and *Paramecium*, also have N termini with some homology to *Pcalp*. Bootstrap analysis and domain composition indicate that *Pcalp* belongs to a distinct clade of calpains that is restricted to *Apicomplexa* and other alveolates (Fig. 1). The diatom *Thalassiosira pseudonana*, which belongs to the chromalveolate kingdom, has an encoded calpain with distant N-terminal homology to the alveolate sequences (not shown).

***Pcalp* Is Expressed in Early Intraerythrocytic Stages.** Because published *Pcalp* mRNA assessments differ from each other (9, 10), we analyzed cDNA by semiquantitative RT-PCR through asexual development. Amplifying both the N-terminal and C-terminal

Author contributions: I.R. and D.E.G. designed research; I.R., A.O., and B.V. performed research; I.R. and D.E.G. analyzed data; and I.R. and D.E.G. wrote the paper.

The authors declare no conflict of interest.

This article is a PNAS Direct Submission.

Freely available online through the PNAS open access option.

Data deposition: The sequences reported in this paper have been deposited in the GenBank database (accession nos. EF432831, EF432832, and EF432833).

¹To whom correspondence should be addressed. E-mail: goldberg@borcim.wustl.edu.

This article contains supporting information online at www.pnas.org/cgi/content/full/0806926106/DCSupplemental.

© 2009 by The National Academy of Sciences of the USA

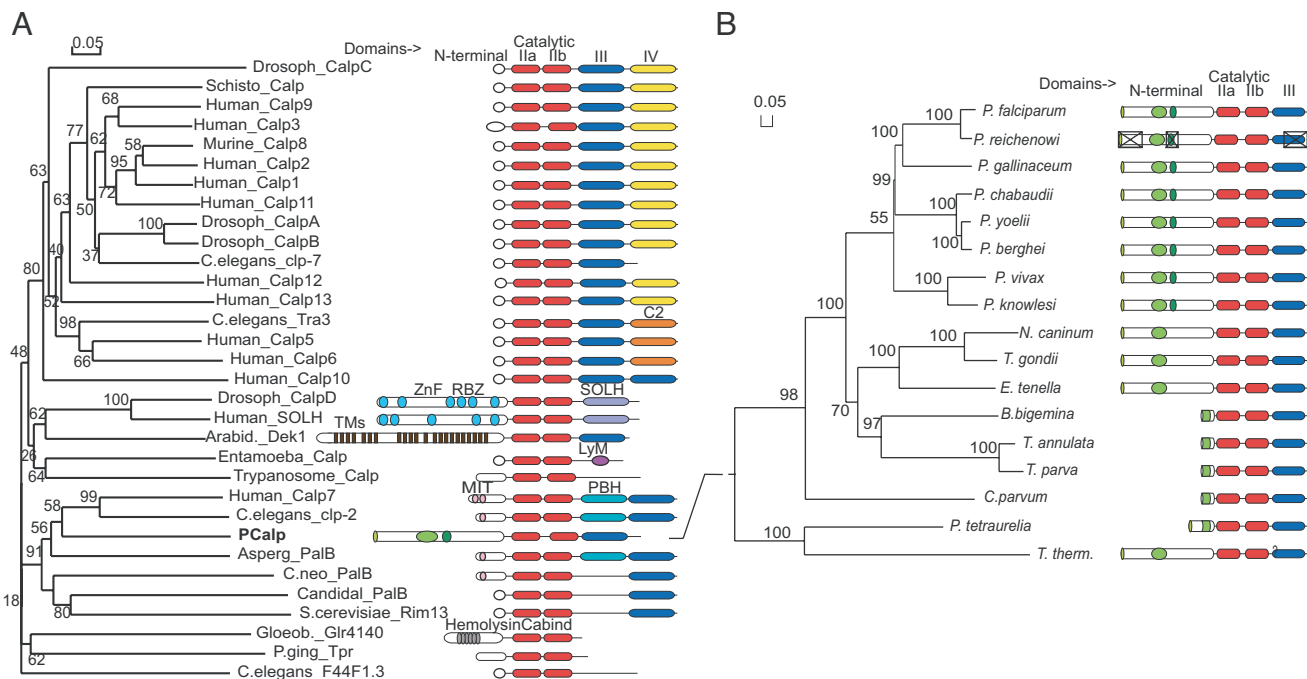


Fig. 1. Phylogenetic analysis reveals Pcalp as a distinct type and clade of calpains. (A) Phylogenetic analysis of Pcalp (catalytic domain) aligned with representatives of each documented type of calpain is shown (left side) together with the domain composition of each protein (right side). Bootstrap values are shown at the tree joints. Domains are color coded and from top to bottom named at their first appearance (SMART code). The Pcalp N terminus has subdomains conserved among *Plasmodium* species (green) (I.R., A.O., and D.E.G., unpublished data). Scale is fractional change per unit distance. (B) Phylogenetic analysis and domain composition of alveolate calpains. Crossed boxes denote incomplete sequence information. Sequence data are listed in [Tables S1 and S2](#) and alignments in [Figs. S1 and S2](#).

coding regions and normalizing against actin, we found a peak of induction (2×) in the late ring/early trophozoite stages [18–24 hours postinvasion (hpi), Fig. 2A], consistent with the data of Bozdech *et al.* (9).

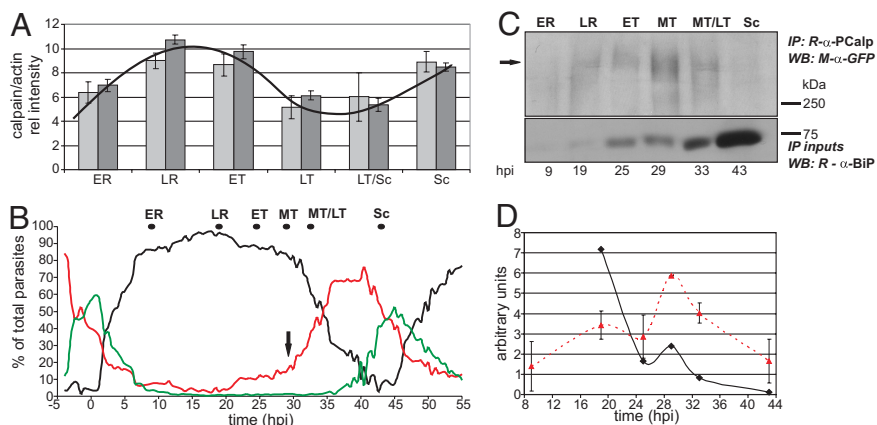
Despite very low expression levels, we were able to detect Pcalp by Western blotting after immunoprecipitation from a large number of parasites (5×10^8). We used a parasite line (C3) in which the endogenous calpain ORF is tagged with GFP (see *Materials and Methods*), so that the anti-GFP antibody could be used for visualization. The asexual cycle was monitored for morphology and DNA content (Fig. 2B). Pcalp was detected from rings through late trophozoites, showing a peak in the amount per cell in midtrophozoites and in concentration (normalized to BiP) in rings (Fig. 2C and D). In these experiments, the majority of the cells entered the

S phase around 30 hpi (Fig. 2B), corresponding to the peak amount of Pcalp.

The Pcalp Gene and Its Activity Are Essential for Optimal Growth. We assessed the essentiality of *Pcalp* for optimal *P. falciparum* asexual growth by using multiple approaches (Fig. 3A). The first one is a classical gene knockout approach using double cross-over with positive/negative selection (11). We used a double positive selection by fusing HcRed to hDHFR and obtained red fluorescent parasites that stably maintained plasmid under drug pressure (Fig. S4). However, we were unable to recover integrants after negative selection despite multiple attempts, assayed by Southern blotting (Fig. 3B) and nested PCR (data not shown).

For gene disruption by 5' single cross-over, we transfected 3D7 parasites with constructs containing 1.3 or 1.6 kb of the 5' end of

Fig. 2. Expression profiles of Pcalp along the asexual cycle. (A) Semiquantitative RT-PCR analysis. Expression of *Pcalp* mRNA in asexual stages was measured by quantifying amplified regions encoding the N (light gray) and C (dark gray) termini (map of region in Fig. S3). The signals were normalized to actin. ER and LR, early and late rings; ET and LT, early and late trophozoites; Sc, schizonts. (B) Time course of Pcalp-GFP (clone C3) cycle. Parasites were sampled every 30 min and analyzed by flow cytometry for DNA content. Populations selected for the analysis are shown in Fig. S3. The percentage of total parasites in pre-S phase, S phase, and mature schizogony are represented by black, red, and green lines, respectively. Dots indicate harvest times for protein analysis (MT, midtrophozoites) and the arrow marks the approximate start of S phase. (C) C3 parasites were harvested at the indicated time points, Pcalp was immunoprecipitated with rabbit anti-Pcalp antiserum and then protein was blotted with mouse anti-GFP antibody. BiP content was also measured. Each lane corresponds to equivalent cell numbers at different stages. (D) Pcalp levels were quantified from blots and plotted with time as absolute values (red) and ratio of calpain to BiP (black). The first point of the ratio is omitted because of minimal BiP expression in early rings.



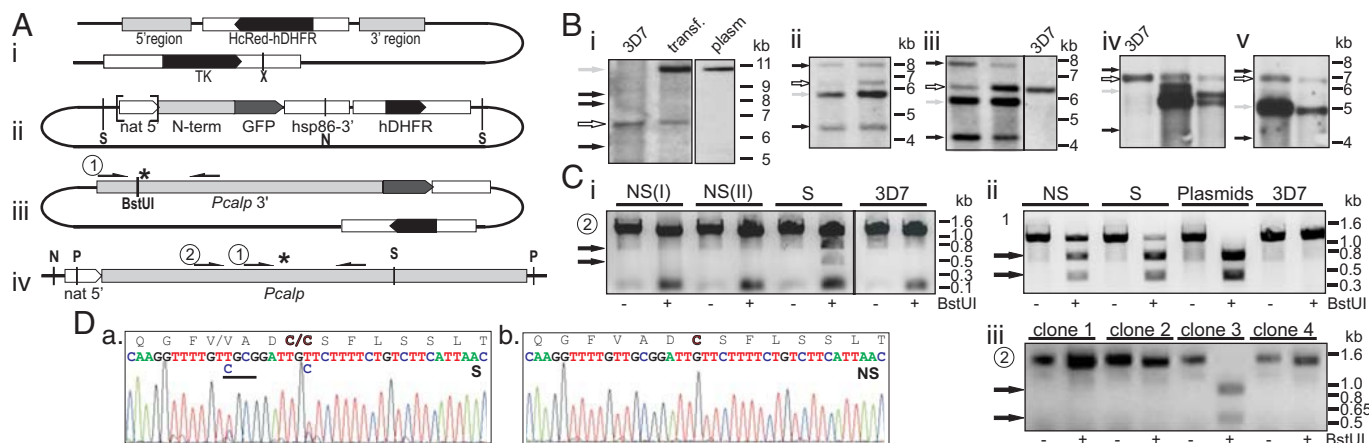


Fig. 3. Attempted genetic strategies to disrupt calpain functionality. (A) Diagrams of the vectors. (i) For double cross-over gene knockout, a positive selection cassette containing HcRed-hDHFR fusion and flanked by *Pcalp* ORF 5' and 3' ends was inserted into a thymidine kinase (TK) negative selection vector. (ii) For single cross-over gene disruption, a sequence homologous to *Pcalp* ORF 5' end was cloned upstream to hDHFR cassette. Two different lengths (1.3 and 1.6 kb) were used. Control constructs are identical but contain 733 bp of upstream sequence (nat 5', brackets). (iii) For allelic replacement, a sequence homologous to 3.8 kb of the *Pcalp* ORF 3' end was used for homologous recombination. Two plasmids were created. Both have a mutation creating a new restriction site (BstUI). Two codons downstream in the active site cysteine codon (*), one has a synonymous change, whereas the other has a nonsynonymous change. Predicted products of integration of ii and iii are shown in Fig. S4. (iv) For reference the *Pcalp* gene is shown. Primers used for PCR/restriction in the allelic replacement strategy are indicated (semiarrows). Restriction sites: X, XmaI; N, NsiI; S, SphI; P, PacI. (B) Southern blot analysis. (i) Double cross-over. Transfected parasite DNA (X/P digested) shows the uninterrupted endogenous gene (open arrow) and episomal plasmid (gray arrow), but no evidence of any integration event (filled arrows). Each panel is a different exposure time. (ii–v) Single cross-over. DNA was restricted with N/S. All 4 transfections with the control vector show the predicted integrations (ii and iii; panels are from 2 blots). None of the 4 transfections with the vectors for gene disruption (iv and v) have evidence of integration events (panels are from the same blot). Arrows as in i. 1.6-kb 5' ORF in ii and iv; 1.3-kb 5' ORF in iii and v; nat 5' in ii and iii. 3D7, genomic DNA from the parental isolate. (C) PCR and restriction screening. DNA was prepared from parasite culture transfected with the synonymous (S) or nonsynonymous (NS) vector and selected for integrants. (i) PCR was performed using primer 2 to amplify the transcribed locus but not plasmids. Product was incubated with (+) or without (–) BstUI (below) and arrows indicate the expected fragments. The S vector transfectants showed evidence of upstream cross-over (introduction of the restriction site), but neither of the NS vector transfectant pools did. (ii) PCR was performed using primer 1 to amplify all copies (including plasmid) from transfectants as well as isolated plasmids (1:1 mix of S and NS). Both isolated and transfected episomal plasmids are restrictable. 3D7, as in B. (iii) Examples of isolated S clones. PCR was performed with primer 2; 1 of the 4 clones shown has crossed-over upstream. (D) Sequencing of PCR products amplified from S (i) and NS (ii) integrant pools. Results of control sequence analysis of plasmids and wild-type genomic amplicons are in Fig. S4.

Pcalp (Fig. 3Aii). As controls we used a second pair of constructs, identical to the previous ones but including an additional 733 bp upstream of the *Pcalp* ORF. These controls, upon integration, recapitulate a functional 5' UTR ahead of the full *Pcalp* ORF, whereas the disruption constructs are designed to generate a promoterless ORF in addition to the truncated copy. All transfections were repeated twice and each resulted in transformants that were subjected to selection for integrants. Although the promoter-containing constructs showed clear integration (Fig. 3Bii and iii), no integration was detectable for the promoterless constructs (Fig. 3Biv and v). These results strongly suggest that *Pcalp* is essential for parasite growth. The data also imply that the 733 bp upstream of the ORF is adequate to drive calpain expression and to maintain viability.

To further assess *Pcalp* essentiality and determine if proteolytic activity of the enzyme is required, we generated 2 almost identical allelic replacement plasmids carrying the 3'-most two-thirds of the *Pcalp* ORF (Fig. 3Aiii). Two mutations were made. The first, common to both plasmids, was a silent mutation that creates a new restriction site. The second mutation, 2 codons downstream at the catalytic cysteine triplet, was either synonymous (S) or nonsynonymous (NS) (Cys>Ala). We transfected 3D7 parasites and selected for integrants. Cross-over can occur upstream or downstream of the catalytic cysteine codon. Assuming that cross-over is random over the 3,815 bp of homologous sequence, the probability of integration upstream of the new restriction site is 22%, downstream of the active site codon is 78%, and between them is 0.16%. When we specifically PCR-amplified the transcribed calpain locus, the only BstUI-restrictable product derived from the S mutation integrant pool (Fig. 3Ci), indicating that upstream cross-over occurs only when the active site cysteine is not changed. We also directly sequenced the amplicons and did not detect NS mutation at the

active site, whereas about one-third of the S mutation pool had an alteration at this codon (Fig. 3D). As a control, we amplified and digested the active site region of the parental 3D7 genome, and the 2 plasmids as isolated DNA and as episomes after transfections (Fig. 3Cii). We confirmed the absence of restrictability in the parental genome, the introduction of the BstUI sensitivity due uniquely to the plasmids, and the similarity in DNA content among the selected transfectants.

We completed our study by isolating clones from each of the transfections to better quantify the proportion of upstream integrants. We isolated nearly 100 clones and screened for PCR product restrictability, as described above (examples in Fig. 3Ciii). Out of 62 NS mutation plasmid-transfected clones, we detected none with upstream integration, whereas $\approx 21\%$ of those isolated from the S mutation transfection carried a newly introduced restriction site and consequently a mutated cysteine codon. These data indicate that the essentiality of *Pcalp* depends on its proteolytic activity. Results of all attempts are summarized in Table 1.

Conditional Knockdown of *Pcalp*. Since disruption of the calpain gene was unachievable, to study the function of the protein in vivo we attempted to generate a conditional knockdown, taking advantage of the FKBP destabilization domain system (12). The 10-kDa FKBP domain, when fused to a protein of interest, targets it for degradation. However, in the presence of the small-molecule FKBP ligand, Shld1, degradation is mitigated. This system has been shown to work in *Plasmodium* for episomally expressed constructs (13). To create a conditional protein knockdown, we tagged the *Pcalp* C terminus with GFP-FKBP by homologous recombination at the 3' end of the endogenous locus (Fig. 4A). After drug cycling with culture constantly exposed to 0.5 μ M Shld1, we obtained successful integration (Fig. 4B). Clones were isolated and a representative one, A7, was chosen for further study.

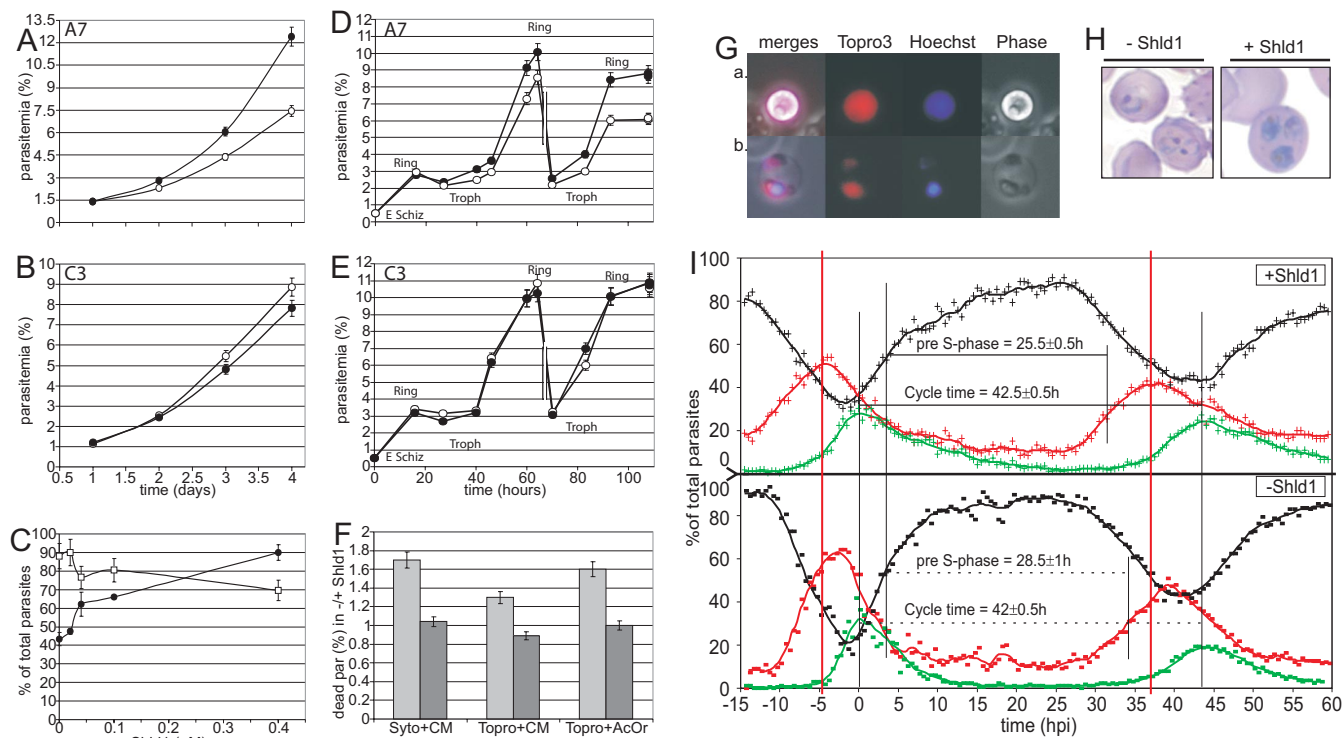


Fig. 5. Analysis of Pcalp knockdown phenotypes. (A and B) Asynchronous cultures of representative clone A7 (A) or C3 (B) were grown with (●) or without (○) 0.4 μM Shld1 and monitored over time by flow cytometry. X axis in A same as in B. (C) Growth of Pcalp-GFP-FKBP (mean of 3 clones, ●) or C3 (□) over 3 days in different Shld1 concentrations. (D and E) Fine analysis of the Shld1 growth phenotype in synchronized cultures of A7 (D) and C3 (E). Schizonts from a culture grown in 0.2 μM Shld1 were isolated and allowed to invade fresh RBCs in the presence (●) or absence (○) of Shld1. The breaks indicate an equal subculture event for each culture. X axis in D same as in E. (F) Viability measurements using different dyes to measure dead parasites in A7 (light) and C3 (dark) cultures. The ratio $-/+$ 0.2 μM Shld1 is plotted. Flow profiles are in Fig. S5. (G) Appearance of A7 dead parasites (Topro3-positive) by fluorescence microscopy. In the absence of Shld1 a unique dead species was detected: trophozoites that are either extraerythrocytic (a) or within RBC ghosts (b). (H) Giemsa-stained thin smears showed a delay in the morphological transition from ring to trophozoite in synchronized A7 cultures in the absence of Shld1. (I) Representative cycles of A7 with (Upper) and without (Lower) Shld1. Cycle points were acquired every 30 min for ≈ 6 days, samples were fixed, and DNA content was analyzed by flow cytometry (Fig. S3). Green, mature schizonts; red, S phase; black, pre-S phase (G₁). The cycle time is shown as distance between the 2 peaks of schizonts; the length of pre-S phase is the time separating the initial slope half maxima of the pre-S-phase and S-phase peaks. Red vertical lines indicate S-phase maxima in +Shld1 for visual comparison to -Shld1 culture. A consistent delay in the start of the S phase was detected when calpain was destabilized.

Multiple efforts to generate a parasite clone lacking calpain expression failed, strongly suggesting that the absence of this gene is incompatible with optimal viability during blood stages. We used 3 different techniques. The double cross-over gene knockout approach failed to generate recombinants. Disruption by single cross-over at the 5' end of the endogenous locus, including a control for homologous recombination, is a new approach. Only when the native promoter was recapitulated did the recombination result in viable parasites. It is always possible that technical problems led to failure to isolate gene-disrupted recombinants for these 2 procedures. Therefore, we designed a third approach, an allelic replacement, to overcome this limitation. We were readily able to isolate parasites with cross-overs upstream of the active cysteine codon, at the predicted frequency, when the vector contained a synonymous active site mutation. In contrast, all recombinants were downstream when the nonsynonymous mutation vector was used. Unlike the first 2 strategies, the allelic replacement method generates recombinants even with the missense mutation vector. It is the site of recombination that informs us of the gene essentiality. In addition, the importance of the active site residue informs us that Pcalp activity is necessary for asexual cycle development.

These studies give us insight into essentiality but do not help us understand the role of the enzyme in the cell. To pursue this, we developed a method, based on the FKBP degradation domain (12, 13), to generate a regulated knockdown of Pcalp. By fusing a GFP-FKBP tag at the endogenous locus we generated clonal lines

in which calpain stability is regulated by the small molecule Shld1. Destabilization of Pcalp yielded a growth defect of 40–60% over 2 cycles. We measured a delay of entry into S phase. Morphologically, the transition from ring to trophozoite was also delayed. Concomitantly we detected an increased number of nonviable parasites. Peaks of Pcalp transcription and translation in normal parasites were seen in the pre-S-phase stages (ring to mid trophozoite), after which a sudden drop in levels was detected. This correlates nicely with the observed knockdown phenotype.

In the absence of Shld1, the fusion protein is degraded, resulting in a knockdown effect. The remarkably scarce transcript and barely detectable protein levels provided challenges in the detection and study of this calpain. The normal level of calpain is so low that we cannot quantify precisely the extent of protein diminution. However, other FKBP fusions have shown a one order of magnitude range in response to Shld1 (ref. 13 and I.R., unpublished results). Assuming that the small number of calpain molecules has a normal Gaussian distribution in all cells, we attribute the death phenotype to those cells (about 20% of the parasites) where the number of calpain molecules is insufficient to overcome the efficiency of the degradation process. Therefore, these cells die because of a loss of calpain function. The rest of the cells may produce just enough calpain to survive, although they show a defect in pre-S-phase development. The total cell cycle time is normal for surviving parasites, suggesting that they are able to catch up. Perhaps a cycle clock further along is able to proceed at the normal time, whereas

Pcalp affects a previous one. Involvement of a calpain-like activity in $G_1 \rightarrow S$ transitions has been suggested in other systems on the basis of indirect evidence (14, 15). An S-phase delay has also been observed in *P. berghei* parasites lacking 1 of 2 *eEF1a* genes, but in that case, the total cell cycle was prolonged (16). Given the role in cell cycle progression, it is interesting that this enzyme is found in the nucleolus (I.R., A.O., and D.E.G., unpublished data), which, in addition to rRNA synthesis and ribosome assembly, has key functions in cell cycle regulation (17). In conclusion, by developing a method for regulated knockdown of Pcalp, we can begin to define its cellular role and further develop this interesting target for antiparasitic chemotherapy.

Materials and Methods

Reagents. Polydonal antiserum (no. 19) was raised in rabbits against Pcalp peptide 41–54. We also used rabbit anti-GFP ab6556 (Abcam), mouse anti-GFP JL8 (BD), rabbit anti-BiP (MR4), and rabbit anti-plasmeprin II (18) antibodies. All other reagents were purchased from either Sigma or NEB unless indicated.

Cell Cultures and Transfection. *P. falciparum* (3D7) was cultured as previously described (19). Parasite synchronization was obtained by using 5% D-sorbitol treatment (20), Percoll (21), and magnetic separation (22). For transfections, 160 μ l of 50% RBCs was transfected by electroporation (23) with \approx 100 μ g of purified vector DNA and then infected with 3D7 schizonts. After 72–90 h, 10 nM WR99210 was added to the medium. To select for integration, parasites were cycled twice on/off drug (24). Double cross-over recombination was selected as described in ref. 11.

Sequence and Phylogenetic Analysis. See *SI Materials and Methods*.

Construction of Vectors. Genomic DNAs were extracted from *P. falciparum* by using a Blood Mini Kit (Qiagen). Primers and restriction sites are listed in Table S3. All cloning steps were confirmed by sequencing. For the gene knockout strategy, the plasmid pHHTK (11) was modified by inserting the HcRed coding region upstream to hDHFR. Into this backbone, we cloned the 5' and 3' ends of the *Pcalp* ORF. Four constructs were made for gene disruption by single cross-over. The calpain N-terminal coding regions (1.3 and 1.6 kb) with or without 733 bp of 5' UTR were PCR amplified from genomic DNA and cloned in pPM2GT (25). The vectors for allelic replacement were generated by cloning 3.8 kb of *Pcalp* 3' ORF into pPM2GT (25). Mutagenesis of the allelic replacement vectors was done with the QuikChange kit (Stratagene). The vectors for 3' tagging were constructed by cloning 1.1 kb of the 3' *Pcalp* ORF into pPM2GT (25) to generate Pcalp-GFP or replacing GFP with GFP-FKBP to generate Pcalp-GFP-FKBP. The FKBP domain was amplified from pBMN YFP-L106P (12).

Semiquantitative RT-PCR. 3D7 RNA was collected from saponin-released parasites by using TRIzol reagent following the manufacturer's protocol (Invitrogen). RNA was collected at 6 stages of development, ER (6–10 hpi), LR (12–18 hpi), ET (20–24 hpi), LT (24–28 hpi), LT/Sc (28–32 hpi), and Sc (34–40 hpi). Stages were

determined according to time and morphological analysis by Giemsa staining. RNA was treated with DNase I (Gibco) and checked by PCR for purity. *Pcalp* cDNA was amplified by one-step RT-PCR with SuperScript (Invitrogen). The RT-PCR products of at least 2 independent reactions for each time point were analyzed on ethidium bromide/agarose gels. Band intensity was in a linear range. Primers are in Table S3.

Southern Blots. For Southern blots, 1 μ g of DNA was digested and analyzed as previously described (25). The double cross-over integrations were screened by *PacI/XmaI* digestion and probed using *Pcalp* ORF 5' end. The single cross-over integrations were screened by *NsiI/SphI* digestion and probing with *Pcalp* ORF 5' or 3' end.

Western Blots. Protein analysis to detect Pcalp after immunoprecipitation was conducted as described in *SI Materials and Methods*.

Microscopy Techniques. Live parasites were observed in the presence of Hoechst 33342 and Topro3. Images were collected with an Axioskop epifluorescence microscope (Zeiss) as described elsewhere (25).

Flow Cytometry. For cell cycle analysis, highly synchronous 2% hematocrit cultures, at 1% parasitemia, were cultivated in gently rocked Roboflasks (Corning) to ensure cell suspension. An automated system, controlled by 3 timers and composed of 3 synchronized peristaltic pumps and a fraction collector, was set up. Each 30 min, \approx 150 μ l of sample culture was extracted by the system through the flask septum, and each sample was fixed and was collected at 4 °C in a 96-well plate. For subculture, fresh, prewarmed RBCs (2% hematocrit) were added through the septum without removing the flask from the incubator. The fixative solution (1.5 vol per sample) was 3.2% formaldehyde and 0.01% glutaraldehyde in PBS. After 5 min of permeabilization with 0.1% Triton X-100 and 15 min of incubation with \approx 75 μ g/ml RNase A, cell DNA was stained with 0.5–1 μ M Topro3. The analysis was conducted on a BD FACSCanto flow cytometer, monitoring fluorescence profiles of infected RBC (Fig. S3).

For viability analysis, we used the following dyes in pairs: 1.25 μ g/ml Cell tracker-green (CM-green), 2.5 μ M Syto59, 0.5 μ M Topro3, and 0.4 μ g/ml AcOr (Molecular Probes). Metabolically active cells incorporated CM-green during a 15-min incubation at 37 °C. Then they were analyzed by flow cytometry in the presence of DNA dyes, cell-permeant Syto59, or cell-impermeant Topro3. The third viability measurement was based on the use of 2 DNA dyes at the same time, AcOr and Topro3. Control dead cells were produced by fixing some of the culture. The analysis was conducted recording the green and far-red fluorescence profiles of infected RBCs (Fig. S5).

ACKNOWLEDGMENTS. We thank the Sanger and Broad Institutes for DNA sequences; Jacobus Pharmaceutical for WR99210; T. Wandless (Stanford University, Palo Alto, CA) for Shld1 and ddFKBP; MR4 and J. H. Adams (University of South Florida, Tampa, FL) for anti-BiP; A. Cowman (Walter and Eliza Hall Institute of Medical Research, Melbourne) for pHHTK; C. Armstrong (Washington University, St. Louis) for sharing results before publication; and M. Drew for critical reading of the manuscript. This work was supported by National Institutes of Health Grant AI-047798.

- Rosenthal PJ (2004) Cysteine proteases of malaria parasites. *Int J Parasitol* 34:1489–1499.
- Wu Y, Wang X, Liu X, Wang Y (2003) Data-mining approaches reveal hidden families of proteases in the genome of malaria parasite. *Genome Res* 13:601–616.
- Croall DE, Ersfeld K (2007) The calpains: Modular designs and functional diversity. *Genome Biol* 8:218.
- Goll DE, Thompson VF, Li H, Wei W, Cong J (2003) The calpain system. *Physiol Rev* 83:731–801.
- Sorimachi H (2004) *Handbook of Proteolytic Enzymes* (Elsevier, London), pp 1206–1225.
- Sorimachi H, Suzuki K (2001) The structure of calpain. *J Biochem (Tokyo)* 129:653–664.
- Perrin BJ, Huttenlocher A (2002) Calpain. *Int J Biochem Cell Biol* 34:722–725.
- Blanchard H, et al. (1997) Structure of a calpain Ca^{2+} -binding domain reveals a novel EF-hand and Ca^{2+} -induced conformational changes. *Nat Struct Biol* 4:532–538.
- Bozdech Z, et al. (2003) The transcriptome of the intraerythrocytic developmental cycle of *Plasmodium falciparum*. *PLoS Biol* 1:E5.
- Le Roch KG, et al. (2003) Discovery of gene function by expression profiling of the malaria parasite life cycle. *Science* 301:1503–1508.
- Duraisingh MT, Triglia T, Cowman AF (2002) Negative selection of *Plasmodium falciparum* reveals targeted gene deletion by double cross-over recombination. *Int J Parasitol* 32:81–89.
- Banaszynski LA, Chen LC, Maynard-Smith LA, Ooi AG, Wandless TJ (2006) A rapid, reversible, and tunable method to regulate protein function in living cells using synthetic small molecules. *Cell* 126:995–1004.
- Armstrong CM, Goldberg DE (2007) An FKBP destabilization domain modulates protein levels in *Plasmodium falciparum*. *Nat Methods* 4:1007–1009.
- Janosy J, et al. (2004) Calpain as a multi-site regulator of cell cycle. *Biochem Pharmacol* 67:1513–1521.
- Zhang W, Lu Q, Xie ZJ, Mellgren RL (1997) Inhibition of the growth of WI-38 fibroblasts by benzyloxycarbonyl-Leu-Leu-Tyr diazomethyl ketone: Evidence that cleavage of p53 by a calpain-like protease is necessary for G_1 to S-phase transition. *Oncogene* 14:255–263.
- Janse CJ, et al. (2003) Malaria parasites lacking *eEF1a* have a normal S/M phase yet grow more slowly due to a longer G1 phase. *Mol Microbiol* 50:1539–1551.
- Boisvert FM, van Koningsbruggen S, Navascues J, Lamond AI (2007) The multifunctional nucleolus. *Nat Rev Mol Cell Biol* 8:574–585.
- Francis SE, et al. (1994) Molecular characterization and inhibition of a *Plasmodium falciparum* aspartic hemoglobinase. *EMBO J* 13:306–317.
- Trager W, Jensen JB (1976) Human malaria parasites in continuous culture. *Science* 193:673–675.
- Lambros C, Vanderberg JP (1979) Synchronization of *Plasmodium falciparum* erythrocytic stages in culture. *J Parasitol* 65:418–420.
- Dluzewski AR, Ling IT, Rangachari K, Bates PA, Wilson RJ (1984) A simple method for isolating viable mature parasites of *Plasmodium falciparum* from cultures. *Trans R Soc Trop Med Hyg* 78:622–624.
- Paul F, Roath S, Melville D, Warhurst DC, Osisanya JO (1981) Separation of malaria-infected erythrocytes from whole blood: Use of a selective high-gradient magnetic separation technique. *Lancet* 2:70–71.
- Fidock DA, Wellems TE (1997) Transformation with human dihydrofolate reductase renders malaria parasites insensitive to WR99210 but does not affect the intrinsic activity of proguanil. *Proc Natl Acad Sci USA* 94:10931–10936.
- Wu Y, Kirkman LA, Wellems TE (1996) Transformation of *Plasmodium falciparum* malaria parasites by homologous integration of plasmids that confer resistance to pyrimethamine. *Proc Natl Acad Sci USA* 93:1130–1134.
- Klemba M, Beatty W, Gluzman I, Goldberg DE (2004) Trafficking of plasmeprin II to the food vacuole of the malaria parasite *Plasmodium falciparum*. *J Cell Biol* 164:47–56.